Biochemistry

 Volume 40, Number 18 May 8, 2001

Accelerated Publications

Kinetic Analysis of Three Activated Phenylalanyl Intermediates Generated by the Initiation Module PheATE of Gramicidin S Synthetase

Lusong Luo and Christopher T. Walsh*

Department of Biological Chemistry and Molecular Pharmacology, Harvard Medical School, 240 Longwood Avenue, Boston, Massachusetts 02115

Received February 27, 2001; Revised Manuscript Received March 26, 2001

ABSTRACT: The three-domain initiation module PheATE (GrsA) of *Bacillus brevis* gramicidin S synthetase catalyzes the activation, thiolation and epimerization of L-phenylalanine (L-Phe), the first amino acid incorporated into the decapeptide antibiotic gramicidin S. There are three activated intermediates in the PheATE catalyzed chemical pathway: L-phenylalanyl-adenosine-5′-monophosphate diester (L-Phe-AMP), L-Phe-S-4′-phosphopantetheine(Ppant)- and D-Phe-S-4′-Ppant-acyl enzyme. In this study, we examined PheATE in single-turnover catalysis using rapid chemical quench techniques. Kinetic modeling of the process of disappearance of the substrate L-Phe, transient appearance and disappearance of L-Phe-AMP and the ad seriatim formation and equilibration of the L- and D-Phe-S-Ppant-acyl enzyme adducts allowed evaluation of the microscopic rate constants for the three chemical reactions in the initiation module PheATE. This study provides the first transient-state kinetic analysis of a nonribosomal peptide synthetase (NRPS) module.

The cyclic decapeptide antibiotic gramicidin S is assembled by a two-subunit (GrsA, GrsB)[1] multimodular enzyme, gramicidin S synthetase, which incorporates five amino acids via the thiotemplate mechanism (*2*−*5*). The chain is initiated on the GrsA subunit (Figure 1), which activates and epimerizes L-Phe into a D-Phe-S-phosphopantetheinyl (P-pant)-enzyme intermediate (*6*, *7*). The 126 kDa GrsA subunit has three identifiable domains (see Figure 1). The most N-terminal is an adenylation (A) domain for L-Phe recognition and ATP dependent activation of L-Phe to L-phenylalanyl-adenosine-5′-monophosphate diester (L-Phe-AMP). The thiolation (T) domain (also known as peptidyl carrier protein, or PCP domain) is a 10 kDa autonomously folding domain that becomes posttranslation-

† This work has been supported by the National Institutes of Health (Grant GM20011 to C.T.W.).

* To whom correspondence should be addressed. Phone: (617) 432 1715. Fax: (617) 432 0438. E-mail: christopher_walsh@hms.harvard.edu.

[1] Abbreviations: GrsA, Gramicidin S synthetase A; GrsB, Gramicidin S synthetase B; L-Phe, L-phenylalanine; Ppant, 4′-phosphopantetheine; aa-S-Ppant-T, aminoacylated thioester form of cofactor Ppant-modified holo T domain; A, adenylation domain; T, thiolation domain; E, epimerization domain; ATE, adenylation-thiolation-epimerization domains; L-Phe-AMP, L-phenylalanyl-adenosine-5′-phosphate diester; AMP, adenosine 5′-monophosphate; ADP, adenosine 5′-diphosphate; ATP, adenosine 5′-triphosphate; TEA, triethylamine; Hepes, *N*-(2-hydroxyethyl)piperzine-*N*′-2-ethanesulfonic acid; NMR, nuclear magnetic resonance; Pi, inorganic phosphate; PPi, inorganic pyrophosphate; PPi-ase, inorganic pyrophosphatase; MesG, 2-amino-6-mercapto-7-methylpurine ribonucleoside; PNP, purine nucleoside phosphorylase; BSA, bovine serum albumin; C, condensation domain; CoA or CoASH, coenzyme A; HPLC; high-performance liquid chromatography; LSC, liquid scintillation counting; TCEP, tris-(2-carboxyethyl)phosphine; TCA, trichloroacetic acid; TLC, thin-layer chromatography; NRPS, nonribosomal peptide synthetase; MALDI-TOF MS, matrix-assisted laser desorption ionization time-of-flight mass spectrometry.

10.1021/bi015518+ CCC: $20.00
Published on Web 04/12/2001

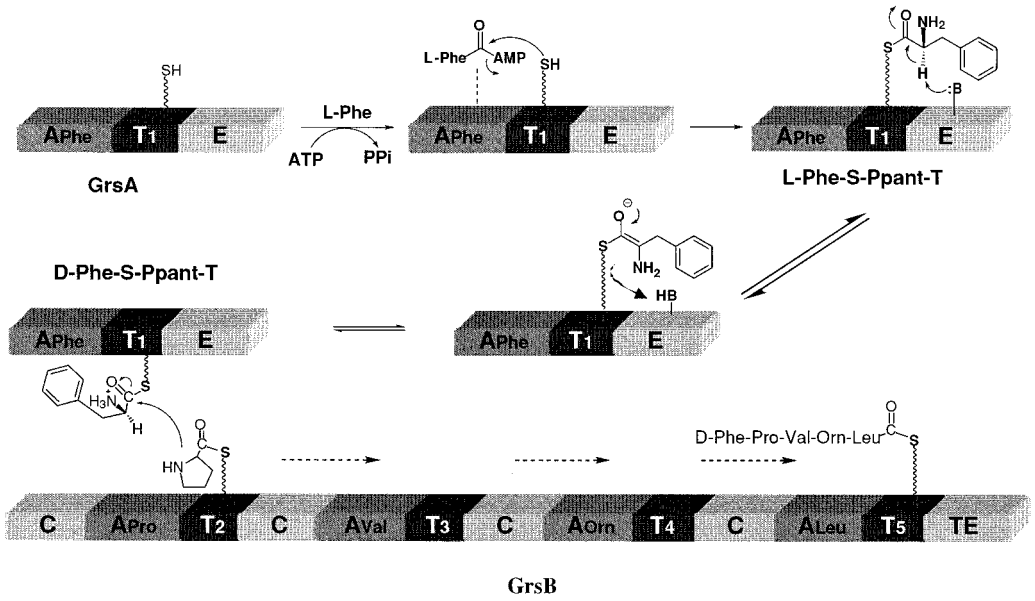

FIGURE 1: Action of the initiation module PheATE of the gramicidin S synthetase. The tightly bound intermediate L-Phe-AMP is formed by the adenylation of L-Phe with ATP·Mg^{2+} catalyzed by the A domain. The amino acyl group is transferred from the L-Phe-AMP intermediate to the phosphopantetheinyl arm of the T domain and subsequently epimerized at the active site of the E domain in the amino acyl-P-pant-acyl enzyme form, giving a 2:1 equilibrium mixture of D-/L-Phe-S-P-pant enzyme adducts. Only the D-isomer is accepted by the downstream condensation domain for transfer to the next module ProCAT in GrsB and then continues the subsequent elongation steps.

ally primed with phosphopantetheine (*5*, *7*) and can then be covalently loaded on its HS-Ppant-prosthetic group with L-Phe to give the L-Phe-S-Ppant-T intermediate. The third domain is a 54 kDa epimerase (E) domain, responsible for equilibrating the Cα-configuration of the Phe moiety in the Phe-S-enzyme to produce 1.9/1 D-Phe-/L-Phe-S-enzyme mixture (*8*). Chain elongation then follows on the four modules of the GrsB subunit, presumably to a pentapeptidyl-S-enzyme that is subsequently dimerized to a decapeptidyl-S-enzyme and released by cyclization. The first module of the downstream GrsB subunit has a clear preference to the D-Phe-S-enzyme form of GrsA as the donor in making a D-Phe_1-L-Pro_2-S-GrsB enzyme intermediate (*7*−*9*).

The tridomain PheATE initiation module is among the best characterized of any nonribosomal peptide synthetase (NRPS) module: the A domain of the PheATE initiation module has been studied for amino acid selectivity in the activation step by the classical ^{32}PPi-ATP exchange assay (*6*, *7*), its X-ray structure has been solved (*10*) and coding specificity for L-Phe has been analyzed (*11*); the holo-T domain has been covalently loaded with L-Phe (*7*, *9*); the E domain was recently characterized by detailed mutational analysis (*8*). However, essentially no information is available about the rates of any of the processes in the A domain, T domain or E domain, much less the sequential chain transfer between the three domains of this NRPS initiation module. The PheATE module generates three assayable intermediates: the noncovalent but tightly bound L-Phe-AMP and then the two covalent intermediates formed ad seriatim, the L-Phe-S-P-pant-T and the D-Phe-S-P-pant-T domain acyl thioester enzyme covalent adducts. In this study, we report rapid quench analysis and deconvolution of the rate constants for the formation of these three consecutive enzyme-bound intermediates, providing the first detailed kinetic analysis of the catalytic workings of an NRPS module.

EXPERIMENTAL PROCEDURES

General. ApoPheATE protein and H753A mutant were overexpressed and purified as described (*7*, *8*). The protein was obtained in a homogeneous state as judged by SDS−PAGE analysis and dialyzed into 50 mM K^+Hepes buffer [pH 7.5, 1 mM tris-(2-carboxyethyl)phosphine (TCEP)]. Priming of apoPheATE (generation of holoPheATE) was achieved by incubation with CoASH and *Bacillus subtilis* Ppant transferase Sfp (*12*, *13*). Reaction mixtures in assay buffer containing 70 μM apo enzyme, 250 μM CoASH, and 50 nM Sfp were incubated for 60 min at 37 °C. ^{1}H NMR spectra were recorded on a Varian M200 spectrometer at 200 MHz. MALDI-TOF mass spectrometry was carried out using a Perceptive Biosystems Voyager-DE STR mass spectrometer. Analytical HPLC was carried out on a Beckman Gold Nouveau system.

HPLC Analysis of Product Formation in Multiple Turnover Reactions Catalyzed by ApoPheATE. Reactions (50 μL each) contained 50 mM K^+Hepes (pH 7.5), 10 mM L-Phe, 8 mM ATP, 10 mM $MgCl_2$, 2 units of inorganic pyrophosphatase (EC 3.6.1.1, used to drive the reaction forward by hydrolyzing the PPi product) and 4 μM apoPheATE and were incubated at 37 °C and quenched at 30, 60, 90, and 120 min by adding 50 μL of 10% TCA (w/v). A control reaction was carried out under the same conditions except that apoPheATE was not included in the reaction. The precipitated protein was pelleted by centrifugation at 11600g for 10 min. The supernatant was injected onto a reversed-phase HPLC column (VYDAC, C18, 4.6 × 250 mm, 5 μm, 300 Å) for analysis. A methanol gradient (0% B for 2 min, 0 to 66.6% B in 30 min) was employed to elute the column after preequilibration in 100% solvent A at a flow rate of 1 mL/min. Solvent A was 2.5% methanol, 2.5% triethylamine (TEA), 25 mM K^+Pi (adjusted to pH 6.5 with H_3PO_4) and solvent B was 50% methanol, 2.5% TEA, 25 mM K^+Pi (adjusted to pH 6.5 with H_3PO_4). The column eluant was

monitored at UV 254 nm. The retention times of L-Phe, AMP, ADP, and ATP were determined by injecting standards to be 14.0, 13.8, 15.3, and 16.3 min, respectively. A new peak at 20.8 min was observed to increase with the length of reaction time and assigned to L-Phe-AMP. The peak was collected and desalted by ZipTip (from Millipore) and analyzed by MALDI-TOF MS. The identity of the peak as L-Phe-AMP was verified by MALDI-TOF MS (monoisotopic) [M + H]: 494.9 (495.1 calcd).

Preparation of Authentic L-Phe-AMP. L-Phe-AMP was prepared following the reported procedure (*14*). AMP (340 mg, 0.98 mmol) and L-Phe (160 mg, 1.0 mmol) were suspended in water (1.2 mL) and dissolved by addition of 5.2 mL of pyridine and followed by the addition of 90 μL of concentrated HCl. The clear solution was cooled to −10 °C in an acetone:ice bath, and then a solution of dicyclhexylcarbodiimide (DCC, 5.15 g) in 6 mL of pyridine was added and stirred vigorously. After the 4 h reaction in the cold bath (−10 °C), a thick yellow suspension was formed and filtered through a fritted funnel. The filtrate was added to 150 mL of acetone held at −50 °C (dry ice:acetone bath). The resulting precipitate was centrifuged at 15000*g* at 4 °C. The collected solids were transferred onto a 15−20 mm fritted funnel, washed with acetone (3 × 10 mL) and ethyl acetate (2 × 10 mL), and lyophilized overnight to afford a white powder (103 mg, 21%). ^{1}H NMR integrals indicate that the powder consists of a mixture of AMP and Phe-AMP in an approximately 4:6 ratio. ^{1}H NMR (D_2O): 3.564 (m, 1H, Cα-H), 4.176 (m, 2H, ribose 5′-H), 4.267 (m, 1H, ribose 4′-H), 4.434 (m, 2H, PheCH$_2$), 6.035 (d, 1H, 1′-H), 8.370 (s, 5H, aromatic H), 8.602 (s, 1H, 3′-H), 8.626 (s, 1H, 8′-H). MALDI-TOF MS (monoisotopic) [M + H]: 495.3 (495.1 calcd).

Steady-State Kinetic Analysis of L-Phe-AMP Formation by ApoPheATE. A coupled, continuous, spectrophotometric assay for inorganic pyrophosphate (PPi) was employed to detect the rate at which PPi is released into solution (*15*, *16*). Reactions were carried out at 30 °C in 100 μL total volume in a microtiterplate and contained 75 mM Tris, pH 7.5, 10 mM $MgCl_2$, 200 μM 2-amino-6-mercapto-7-methylpurine ribonucleoside (MesG), 0.15 unit of purine nucleoside phosphorylase (PNP), 0.15 unit of inorganic pyrophosphatase (PPi-ase), 2 mM ATP, 2 μM apoATE, and varying concentrations of L-Phe (100−2000 μM). Reactions were initiated by addition of the amino acid substrate after a 10-min incubation to allow the PPi-ase/PNP/MesG couple to remove any contaminating PPi or Pi. A SPECTRA max plus^{384} microplate spectrometer was used to monitor absorbance at 360 nm [$\Delta\epsilon_{360} = 17.6$ mM^{-1} cm^{-1}, as reported in Keating et al. (*15*)] and the software SOFTmax PRO 3.1 was used for data analysis.

Measurement of Single-Turnover Time Course for L-Phe-AMP Formation Catalyzed by ApoPheATE. Single-turnover time courses were measured at 30 °C using a rapid-quench flow apparatus from KinTek instruments. Each reaction was initiated by mixing 15 μL of 70 μM (or 47 μM) apoATE (in 50 mM K^+Hepes, pH 7.5, 10 mM $MgCl_2$, and 1 mM TCEP) and 15 μL of 12 μM L-[^{14}C]Phe (450 mCi/mmol), and 8 mM ATP in 50 mM K^+Hepes buffer (pH 7.5). The final concentration after mixing (total volume 30 μL) were 35 μM (or 23.5 μM) apoPheATE enzyme, 6 μM L-[^{14}C]Phe, 5 mM $MgCl_2$, 4 mM ATP, and 0.5 mM TCEP. After incubation for a specified period of time (0.01−5.0 s), the reaction mixture was quenched with 100 μL 10% TCA (w/v). The quench solution was collected in a 2-mL Eppendorf tube. Following vigorous vortexing the precipitated protein was pelleted by centrifugation for 20 min at 11600g at 4 °C. One microliter of the reaction supernatant was loaded onto a cellulose TLC plate (DC-Plastikfolien, EM Science) and developed in butanol/water/acetic acid; 4:1:1 (v/v) (developing buffer A). The ratio of L-[^{14}C]Phe ($R_f = 0.71$) and L-[^{14}C]Phe-AMP ($R_f = 0.13$) was calculated from the phosphorimage of the TLC plate.

Measurement of Single-Turnover Time Course for HoloPheATE Catalyzed Reactions. Single-turnover time courses for holoPheATE (or H753A mutant) catalyzed adenylation, thiolation, and epimerization of L-[^{14}C]Phe (450 mCi/mmol) or D-[^{14}C]Phe (56 mCi/mmol) were measured in a similar manner as described above except that each reaction was duplicated so that one set of samples were used to measure the absolute radioactivity in the supernatant and pellet and the other set of samples were used to determine the ratio of L-[^{14}C]Phe/L-[^{14}C]Phe-AMP in the supernatant and L-[^{14}C]Phe /D-[^{14}C]Phe cleaved from the enzyme in the pellet. Each reaction was initiated by mixing 15 μL of 70 μM holoPheATE (or H753A mutant) and 15 μL of 12 μM L-[^{14}C]Phe (or D-[^{14}C]Phe) in the same buffer as described above. The final concentrations after mixing (total volume 30 μL) were 35 μM holoPheATE (or H753A mutant) enzyme, 6 μM L-(or D)-[^{14}C]Phe, 5 mM $MgCl_2$, 4 mM ATP, and 0.5 mM TCEP. After incubation for a specified period of time (0.01−8.0 s), the reaction mixture was quenched with 100 μL of 10% TCA (w/v). The quenched solution was collected in a 2-mL Eppendorf tube. Following vigorous vortexing, the precipitated protein was pelleted by centrifugation for 20 min at 11600*g* at 4 °C. For one set of the duplicated samples, the supernatant was separated from the pellet and the pellet washed with 2 × 500 μL of 10% TCA. The supernatant (combined with the solution from two washes) and the pellet (dissolved by formic acid) were assayed by scintillation counting using LS6500 Multipurpose Scintillation Counter (Beckman). For the duplicated set of samples, the supernatant was analyzed on cellulose TLC plates to separate L-[^{14}C]Phe and L-[^{14}C]Phe-AMP using developing buffer A. The precipitates were washed in succession with 1 mL of ether/ethanol [1:3 (v/v)] and 1 mL of ether. The [^{14}C]Phe-S-Ppant-enzyme complexes were hydrolyzed and extracted according to the procedure described in ref *8*. One microliter of sample was applied to chiral TLC plates (Aldrich) in order to separate D- and L-isomers. The TLC was developed in developing buffer B [acetonitrile/water/acetic acid; 4:1:1 (v/v)]. The ratio of L-[^{14}C]Phe ($R_f = 0.59$) and D-[^{14}C]Phe ($R_f = 0.49$) was calculated from the phosphorimage of the chiral TLC plate.

Data Collection and Analysis. Phosphorimages of TLC plates were obtained after 12−96 h exposure to 'BAS−IIIS' image plates and read by a "Bio-Imaging Analyzer BAS1000" (Fuji). The image was analyzed densitometrically using the Image Gauge 3.0 software. All single-turnover progress curve data were fitted to enzymatic mechanistic schemes using the program DYNAFIT by Petr Kuzmic (*17*).

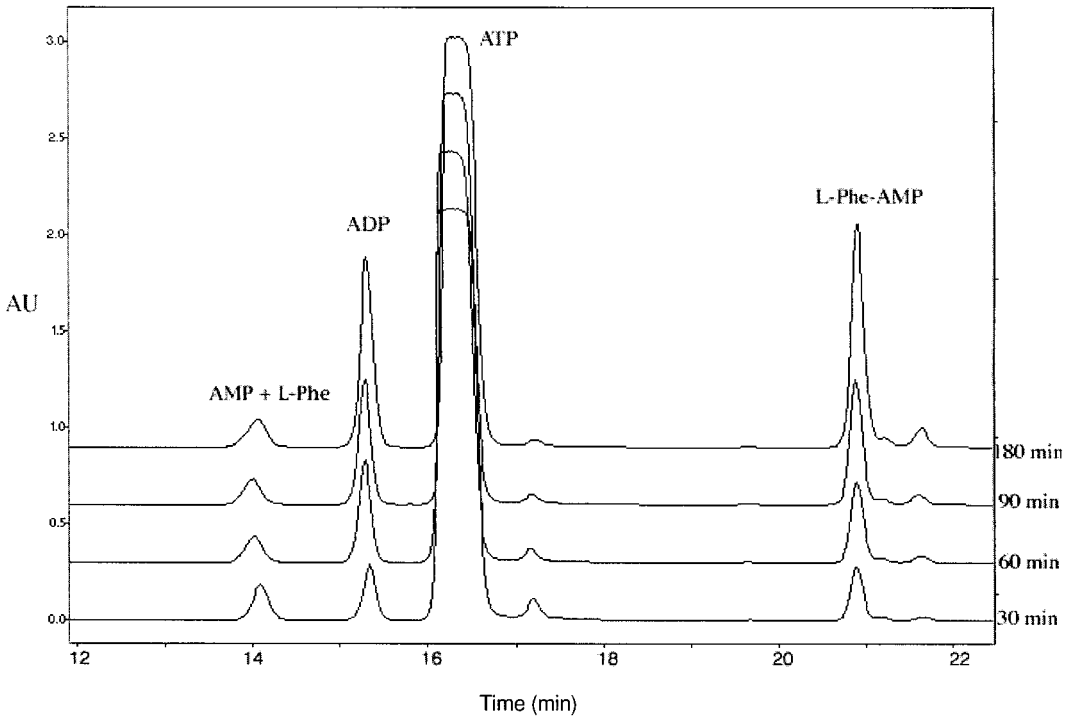

FIGURE 2: HPLC traces of the time-dependent multiple-turnover reaction of 10 mM L-Phe, 8 mM ATP, 10 mM $MgCl_2$, 2 units of inorganic pyrophosphatase, and 4 μM apoPheATE in 50 mM K^+Hepes buffer (pH 7.5) at 37 °C. Reactions were quenched at 30, 60, 90, and 120 min after the reaction started.

RESULTS

Detection of L-Phe-AMP Released as a Product of ApoPheATE-Catalyzed Multiple-Turnover Reaction. Formation of L-Phe-AMP was detected by HPLC analysis of the multiple-turnover reaction catalyzed by apoPheATE with L-Phe in the presence of ATP·Mg^{2+} and inorganic pyrophosphatase. The apoPheATE enzyme lacks the phosphopantetheine prosthetic group so that the subsequent aminoacyl transfer to the T domain could not occur. The HPLC chromatogram of the reaction mixture contains peaks of L-Phe and AMP (14.0 and 13.8 min), ADP (15.3 min),[2] ATP (16.3 min) and a new peak at 20.8 min, which is not observed with the control reaction in the absence of apoPheATE. As shown in Figure 2, this new peak increases with reaction time. MALDI-TOF mass spectroscopic analysis of the collected peak showed a mass peak of [M + H] (monoisotopic) at 494.9 Da, consistent with the calculated Phe-AMP mass at 495.1 Da. The identity of this multiple turnover reaction product was further confirmed by HPLC coelution with a synthetic L-Phe-AMP standard.

Previous studies suggest that A domains of NRPSs such as Gramicidin S synthetase recognize and activate amino acids and covalently aminoacylate the phosphopantetheinyl groups on the T domains (*7*, *15*). The aminoacyl adenylate is proposed to be a labile and tightly bound intermediate for this activation process. The HPLC trace of Phe-AMP accumulation clearly indicates multiple turnovers at a rate of ca. 2.2 μM/min and therefore some loss of the bound aminoacyl-AMP from the A domain active site into solution.

Steady-State Kinetic Analysis of L-Phe-AMP Formation by ApoPheATE. The steady-state rate of apoPheATE catalyzed L-Phe-AMP formation was measured by detecting the PPi release rate using an inorganic pyrophosphatase-based assay. The coupled reaction mixture included PP-iase/PNP/MesG, which allowed the PPi formation to be monitored at 360 nm. The PPi release rate was measured at a slow 0.0067 s^{-1}. Comparison of this net PPi release rate to the Cα-H washout rate (>1.67 s^{-1}) or L-Phe-S-Ppant acyl enzyme epimerization rate (>0.03 s^{-1}) (*8*), which are all indications of the occurrence of the third reaction step (epimerization step of the three sequential reactions), indicates PPi release and thereby Phe-AMP release rates are kinetically incompetent and that release of L-Phe-AMP into solution is off the reaction pathway.

L-Phe-AMP Formation by ApoPheATE under Single-Turnover Reaction Conditions. To determine the actual rate of L-Phe-AMP formation *within* the active site of the PheATE A domain, we turned to single-turnover analysis using rapid-quench techniques in conjunction with the radiolabeled substrate L-[^{14}C]Phe. First the apo form of PheATE was acid-quenched after exposure to ATP and L-[^{14}C]Phe for specified period of time (ms), releasing both unreacted L-[^{14}C]Phe and L-[^{14}C]Phe-AMP into the acidified supernatant (less than 2% radioactivity was trapped in the pellet). Separation of the L-[^{14}C]Phe-AMP and the starting substrate L-[^{14}C]Phe was then achieved by cellulose TLC. The L-[^{14}C]Phe-AMP intermediate was found to be stable at low pH (the quenching mixture had a pH of 0.9 and the developing buffer for cellulose TLC had a pH of 3.0) and no hydrolysis was observed over time. The TLC radio densitometry assay was utilized to quantitate the ratio of L-[^{14}C]Phe and L-[^{14}C]Phe-AMP, with error limits of ±3% as reported by Stachelhaus and Walsh (*8*). Under the two conditions analyzed, enzyme concentration of 23.5 μM (reaction one) and 35 μM (reaction two) was in significant molar excess over the concentration of the limiting substrate L-[^{14}C]Phe (6.0 μM) to restrict

[2] GrsA, like aminoacyl-tRNA synthetases, is able to catalyze AMP → ADP conversion reaction by transfer of the γ-phosphate of ATP to reactive L-Phe-AMP (*1*).

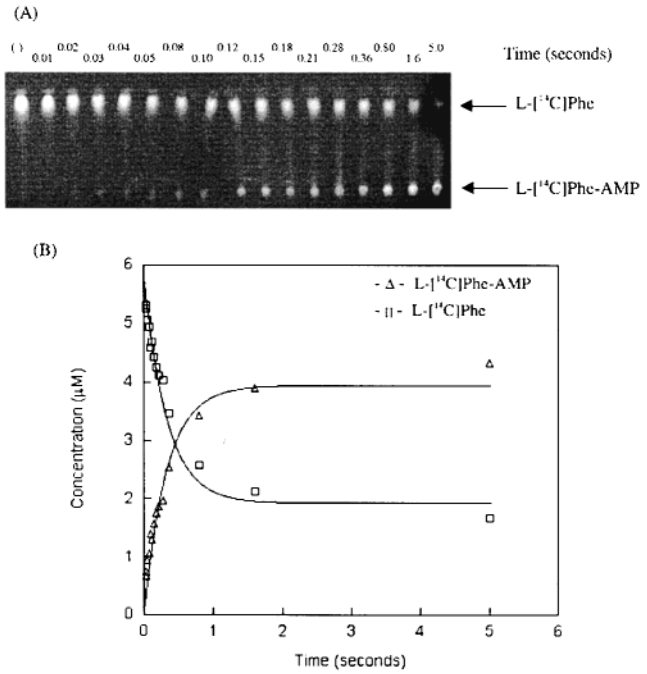

FIGURE 3: (A) Phosphorimage of the cellulose TLC plate analysis of the single-turnover reaction of 35 μM apoPheATE enzyme with 6 μM L-[^{14}C]Phe, 5 mM $MgCl_2$, 4 mM ATP, and 0.5 mM TCEP in 50 mM K^+Hepes, pH 7.5, quenched by a rapid-quench flow apparatus after 0.01, 0.02, 0.03, 0.04, 0.05, 0.08, 0.10, 0.12, 0.15, 0.18, 0.21, 0.28, 0.36, 0.80, 1.6, and 5.0 s. The first lane to the left is a control reaction carried out under the same condition for 5.0 s without enzyme. (B) Time course for the single-turnover progress curve fitted by DYNAFIT. L-[^{14}C]Phe (□) and L-[^{14}C]Phe-AMP (△) are shown with lines from fitting.

reaction to a single turnover of the substrate. The time courses measured for both reaction one (data not shown) and reaction two (see Figure 3) showed that about 75% of the initial L-[^{14}C]Phe was converted to L-[^{14}C]Phe-AMP and the equilibrium was reached after ca. 500 ms. The rate data were fitted to a first-order reaction kinetic model (eq 1) using

$$\text{apoPheATE·L-Phe·ATP·Mg}^{2+} \underset{k_{-1}}{\overset{k_1}{\rightleftharpoons}} \text{apoPheATE·L-Phe·ATP·Mg}^{2+} \quad (1)$$

program DYNAFIT to give the forward and reverse reaction rates. The rates were quite comparable between reaction one ($k_1 = 2.2 \pm 0.1$ s^{-1}, $k_{-1} = 1.1 \pm 0.1$ s^{-1}) and two ($k_1 = 2.0 \pm 0.1$ s^{-1}, $k_{-1} = 1.0 \pm 0.1$ s^{-1}), suggesting that the rates obtained were indeed that of catalysis instead of substrate binding (k_{on} and k_{off}). The 2.0 s^{-1} formation rate of the enzyme-bound L-Phe-AMP in single-turnover reaction conditions is 300-fold faster than the PPi release rate (0.0067 s^{-1}) monitored at steady-state conditions. This result indicates that the slow steady-state, multiple-turnover rate is indeed due to adventitous release and loss of L-Phe-AMP and that single-turnover studies are required to evaluate the formation rate for the L-Phe-AMP in the A domain active site.

Single-Turnover Profile for HoloPheATE Catalyzed Adenylation, Thiolation, and Epimerization Reactions. We next turned to the *holo* form of PheATE, with the prosthetic group installed on the T domain and thereby competent to carry reaction flux forward to the T and E domains. Clearly, steady-state kinetics would not be of much use since the end point is the stoichiometric Phe-S-Ppant-enzyme. Single-turnover rapid quench analysis was thus again utilized, this time to evaluate the three sequential reaction steps, adenylation, thiolation and epimerization of the A, T, and E domains, respectively. The deconvolution of these reaction steps requires the capture of all three intermediates: L-Phe-AMP, L-Phe-S-Ppant-enzyme, and D-Phe-S-Ppant-enzyme. This was achieved as follows: first a TCA precipitation (by rapid quench apparatus) of the reaction mixture to separate radioactive species in the supernatant (L-[^{14}C]Phe and L-[^{14}C]Phe-AMP) from those in the protein pellet (L-[^{14}C]Phe-S-Ppant-enzyme and D-[^{14}C]Phe-S-Ppant-enzyme); the L-[^{14}C]Phe and L-[^{14}C]Phe-AMP in the supernatant were separated using cellulose TLC (Figure 4A); the L-[^{14}C]Phe and D-[^{14}C]Phe released by hydrolysis of the L- and D-Phe-S-Ppant-enzyme covalent intermediates were then separated by chiral TLC (Figure 4B). As shown in Figure 4A, the time-dependent disappearance of substrate L-[^{14}C]Phe and the appearance/disappearance of L-[^{14}C]Phe-AMP are visualized from the cellulose TLC phosphorimage. The falloff of the L-[^{14}C]Phe-AMP is consistent with its conversion to later intermediates. Evaluating the ratio of L-[^{14}C]Phe and L-[^{14}C]Phe-AMP versus time and normalizing for recovery of the overall radioactive counts in supernatant, it is seen that the L-[^{14}C]Phe-AMP first accumulated to its maximum (~20% of the radiolabeled mixture) at about 200 ms and then gradually disappeared as the subsequent intermediates formed. The formation of the L-[^{14}C]Phe-S-Ppant-enzyme and its subsequent transformation to D-[^{14}C]Phe-S-Ppant-enzyme were assessed by quantitation of L- and D-[^{14}C]Phe released by hydrolysis of the acyl enzyme and then separated on chiral TLC (Figure 4B). Clearly, the L-[^{14}C]Phe-S-Ppant-enzyme formed first while the formation of D-[^{14}C]Phe adduct was not observed until 120−150 ms after the reaction started. Over time, the D-[^{14}C]Phe adduct accumulated to higher abundance than the L-[^{14}C]Phe-S-enzyme. A global fitting of the obtained data produced four curves (see Figure 4C), showing L-[^{14}C]Phe disappearance, L-[^{14}C]Phe-AMP rise and fall, and the rise of L-[^{14}C]Phe-S-Ppant-enzyme, then the accumulation of D-[^{14}C]Phe-S-Ppant-enzyme. At equilibrium, about 85% of substrate L-[^{14}C]Phe was converted to enzyme bound forms. About 10% of the enzyme associated L-[^{14}C]Phe was L-[^{14}C]Phe-AMP and of the remainder the D-[^{14}C]Phe-S-Ppant-enzyme/L-[^{14}C]Phe-S-Ppant-enzyme ratio was about 1.5/1. The D-[^{14}C]Phe-S-Ppant-enzyme built up after about 120 ms lag time. A blow up of the early time interval is displayed in Figure 4D. Global fitting of the experimental data to a kinetic model (eq 2) using the program DYNAFIT

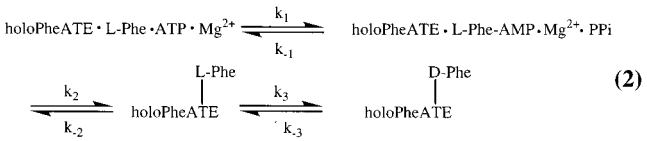

(2)

yielded rate constants (Table 1) for the forward and reverse directions of the following three intermediates (1) L-Phe to L-Phe-AMP are $k_1 = 4.7 \pm 0.5$ s^{-1} and $k_{-1} = 13 \pm 2$ s^{-1}, (2) L-Phe-AMP to L-Phe-S-Ppant-enzyme are $k_2 = 7.9 \pm 0.6$ s^{-1} and $k_{-2} = 2.1 \pm 0.3$ s^{-1}, (3) L-Phe-S-Ppant-enzyme to D-Phe-S-Ppant-enzyme are $k_3 = 2.7 \pm 0.4$ s^{-1} and $k_{-3} = 2.1 \pm 0.3$ s^{-1}.

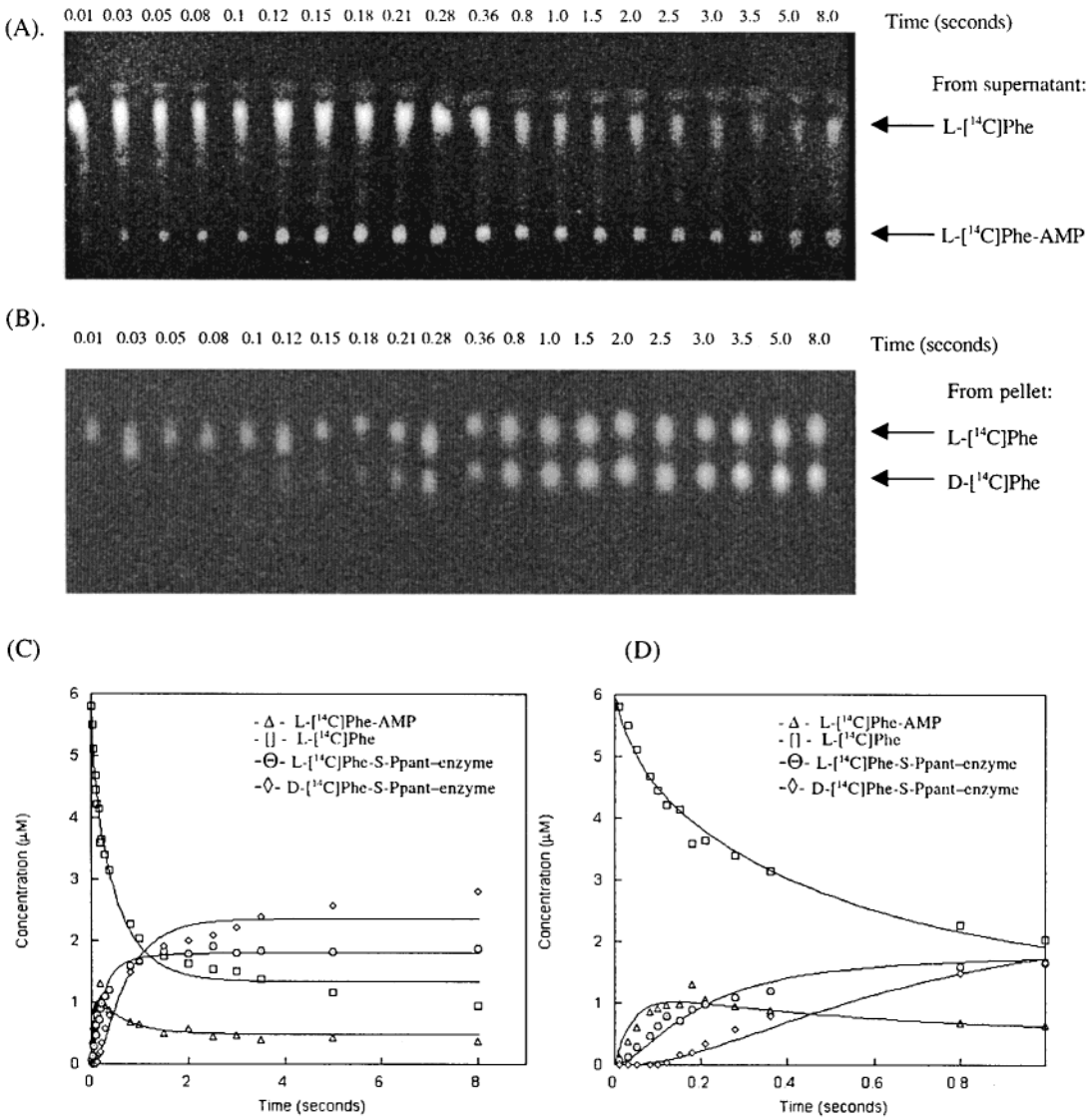

FIGURE 4: (A) Phosphorimage of the cellulose TLC plate analysis of the single-turnover reaction supernatant of 35 μM holoPheATE enzyme with 6 μM L-[^{14}C]Phe, 5 mM $MgCl_2$, 4 mM ATP, and 0.5 mM TCEP in 50 mM K^+Hepes (pH 7.5). (B) Phosphorimage of the chiral TLC plate analysis of the same single-turnover reaction hydrolysis product from pellet. (C) Time course for the single-turnover reaction progress curve fitted by DYNAFIT. (D) Blow-up of the first second of the same single-turnover reaction progress curve. For panels C and D, L-[^{14}C]Phe (□), L-[^{14}C]Phe-AMP (△), D-[^{14}C]Phe-S-Ppant-enzyme (◇) and L-[^{14}C]Phe-S-Ppant-enzyme (⊙) are shown with lines from fitting.

Table 1: Rate Constants for Individual Reaction Steps Catalyzed by HoloPheATE and Mutant H753A

	k_1 (s^{-1})	k_{-1} (s^{-1})	k_2 (s^{-1})	k_{-2} (s^{-1})	k_3 (s^{-1})	k_{-3} (s^{-1})
holoPheATE + L-[^{14}C]Phe	4.7 ± 0.5	13 ± 2	7.9 ± 0.6	2.1 ± 0.3	2.7 ± 0.4	2.1 ± 0.3
holoPheATE + D-[^{14}C]Phe	8 ± 2	39 ± 14	11 ± 1	1.0 ± 0.2	1.8 ± 0.4	2.5 ± 0.6
H753A + L-[^{14}C]Phe	3.3 ± 0.5	8 ± 2	2.8 ± 0.3	0.5 ± 0.1		

Single-Turnover Studies with HoloPheATE Starting from D-[^{14}C]Phe. Although the physiological isomer for the PheATE module is L-Phe, it has been shown that D-Phe can be activated by the A domain (*6*−*8*), allowing us to carry out comparable rapid quench studies, starting from D-[^{14}C]Phe. In particular, this study gives insight into A, T, and E domain action and serves as an independent check for the D-Phe-S-Ppant-enzyme ⇔ L- Phe-S-Ppant-enzyme interconvertion rate constants. A similar kinetic model (eq 3) was used to fit the experimental data, the curves obtained are shown in Figure 5A and the calculated rate constants collected in Table 1. The rate constants of D-[^{14}C]Phe reactions are $k_1 = 8 \pm 2$ s^{-1}, $k_{-1} = 39 \pm 14$ s^{-1}, $k_2 = 11 \pm 1$ s^{-1}, $k_{-2} = 1.0 \pm 0.2$ s^{-1}, $k_3 = 1.8 \pm 0.4$ s^{-1}, and $k_{-3} = 2.5 \pm 0.6$ s^{-1}. With the substrate L-Phe, the equilibrium constant $K_1(k_1/k_{-1})$ was 0.36, which was close to the K_1 value of 0.2 for the D-Phe reaction. This result was consistent with almost equivalent recognition of L- and D-Phe by GrsA (*7*, *8*), although D-Phe gives D-Phe-AMP 2-fold faster and hydrolyzes from D-Phe-AMP 3-fold faster. The forward rate for D-Phe-AMP to D-Phe-S-enzyme

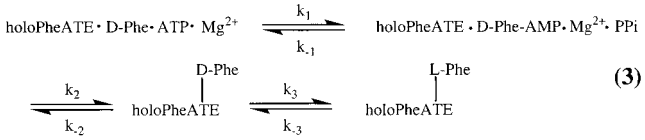

(3)

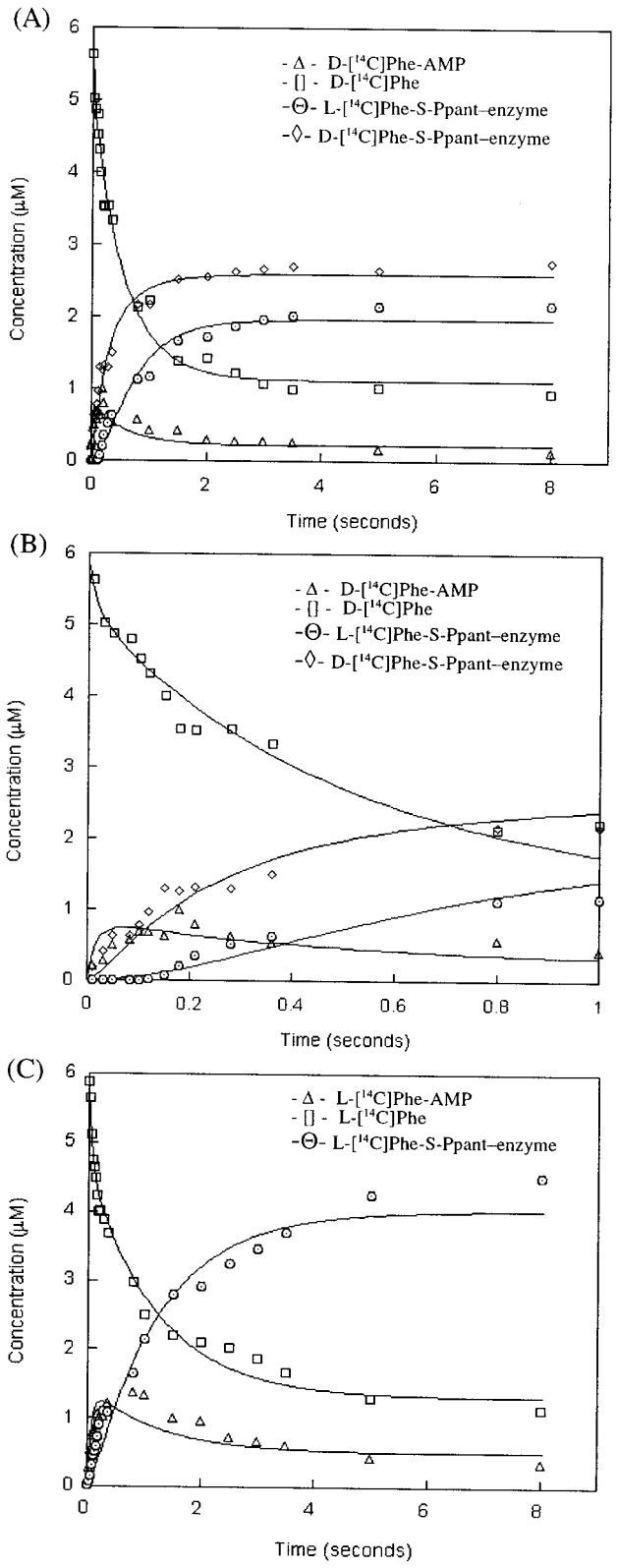

FIGURE 5: (A) Time course for the single-turnover reaction progress curve of 35 μM holoPheATE enzyme with 6 μM D-[^{14}C]Phe, 5 mM $MgCl_2$, 4 mM ATP, and 0.5 mM TCEP in 50 mM K^+Hepes (pH 7.5), fitted by DYNAFIT. (B) Blow-up of the first second time interval of the same single-turnover reaction progress curve. For panels A and B, D-[^{14}C]Phe (□), D-[^{14}C]Phe-AMP (△), D-Phe-S-Ppant-enzyme (◇), and L-Phe-S-Ppant-enzyme (⊙) are shown with lines from fitting. (C) Time course for the single-turnover reaction progress curves of 35 μM H753A mutant enzyme with 6 μM L-[^{14}C]-Phe, 5 mM $MgCl_2$, 4 mM ATP, and 0.5 mM TCEP in 50 mM K^+Hepes (pH 7.5). L-[^{14}C]Phe (□), L-[^{14}C]Phe-AMP (△), L-Phe-S-Ppant-enzyme (⊙) are shown with lines from fitting by DYNAFIT.

is close to that for L-Phe-AMP to L-Phe-S-enzyme (11 s^{-1} vs 7.9 s^{-1}) as are the k_{-2} values. For D-Phe-S-Ppant-enzyme ⟺ L-Phe-S-Ppant-enzyme, we note that the forward reaction rate k_3 with L-Phe as the substrate is almost identical to the reverse reaction rate k_{-3} with D-Phe as the substrate (2.7 s^{-1} vs 2.5 s^{-1}) while the k_3 of the forward D-Phe reaction equals the reverse reaction rate k_{-3} for L-Phe reaction (1.8 s^{-1} vs 2.1 s^{-1}). Based on the fitted results, the equilibrium constants for the epimerization reaction with L-Phe and D-Phe as starting substrate are reversed, with $K_{3L}(k_3/k_{-3}) = K_{-3D}(k_{-3}/k_3)$ (1.3 vs 1.4), indicating a preference for D-Phe-S-Ppant-enzyme as the product at equilibrium regardless of the chirality of the starting substrate. This outcome resulting from kinetic analysis agrees well with previous studies by Stachelhaus and Walsh (*8*). These equivalencies give confidence that the experimental data are accurate and simulations consistent.

Single-Turnover Studies with an E Domain H753A Mutant of HoloPheATE. A similar rapid quench analysis of the single-turnover reaction profile was also carried out on an epimerization domain mutant H753A (PheATE*). H753 residue is the second histidine residue in the His motif (HHxxxDGxS) of the E domain (*8*). Previous site-directed mutagenesis studies of the H753A mutant showed that this residue is crucial for the epimerization reaction, as demonstrated by the inability of the H753A enzyme to exchange the Cα-^{3}H of L-[2,3-$^3H_2$]Phe and its failure to interconvert the L-Phe-S-Ppant-enzyme to D-Phe-S-Ppant-enzyme. As expected in the single turnover analysis, no epimerization reaction was detected in the H753A reaction, only L-Phe-S-Ppant-enzyme forms (Figure 5C). While the L-[^{14}C]Phe-AMP formation and decay rates ($k_1 = 3.3 \pm 0.5$ s^{-1}, $k_{-1} = 8 \pm 2$ s^{-1}) of H753A PheATE mutant were very close to those of the wild-type reaction (Table 1), the forward and reverse thiolation rates were down 3−4-fold. The absence of a catalytically functional E domain has little effect on forward and reverse rates for two prior intermediates, L-Phe-AMP and L-Phe-S-Ppant-enzyme.

DISCUSSION

The complexity of the tridomain structure of the PheATE initiation module of the GrsA nonribosomal peptide synthetase and the generation of three covalent/tightly bound intermediates render the measurement of the steady-state rate of individual steps or combination of steps and also the determination of the partitioning of the enzyme among the three intermediates very difficult. Specifically, the product of the first half reaction of the A domain reaction, L-Phe-AMP, is a hydrolytically labile and tightly bound intermediate while the next substrate for the A domain in the second half reaction is an intramolecular, stoichiometric downstream T domain. Analogously, the substrate for the E domain is L-Phe covalently tethered to the Ppant group from the upstream T domain. In this study, we show that rapid quench studies can be applied to solve and deconvolute the single-turnover profile of the PheATE catalytic pathway. The microscopic rate constants obtained by kinetic modeling and simulation present a clear picture of the kinetic profile for a three step sequential reaction catalyzed by an initiation module of an antibiotic-forming nonribosomal peptide synthetase. This approach could be used to examine the timing of the individual reactions in the assembly line enzyme

catalysis of other NRPS and multimodular polyketide synthetase (PKS) systems (*18*, *19*).

The paired A-T domains in NRPS modules, as in this ATE initiation module of gramicidin S synthetase, function together with the pantetheinyl arm serving as the acceptor cosubstrate in the second half reaction to capture the activated phenylalanyl moiety generated as L-Phe-AMP in the first half reaction. The first half reaction, at $k_1 = 4.7\ s^{-1}$, and the second half reaction at $k_2 = 7.9\ s^{-1}$, are about equivalently fast and under saturation conditions the L-Phe-S-Ppant-enzyme accumulates to a significant fraction. Given the observed release rate of $0.0067\ s^{-1}$ for release of Phe-AMP into solution in multiple turnover cycles of the apoPheATE, one can estimate that 0.0067/7.9 is the comparison for partition of L-Phe-AMP between unproductive loss to solution and productive capture by pantetheinyl arm of the T domain. About 1 Phe-AMP in 1200 catalytic cycles is lost, a reflection of efficient throughput by the paired A and holoT domains.

The generation of tightly held acyl-AMP and aminoacyl-AMP intermediates is also carried out by other superfamilies of adenylation enzymes, including acyl-CoA ligases (*20*) and aminoacyl-tRNA synthetases (*21*). For the acyl-CoA ligases, e.g., 4-chlorobenzoate:CoA ligase, the analogy is most marked in the second step transfer of the activated acyl group of the acyl-AMP to the HS-pantetheinyl arm of coenzyme A rather than the HS-pantetheinyl arm attached to a T domain in NRPS. For 4-chlorobenzoate:CoA ligase, rapid quench studies have revealed the first step at $135\ s^{-1}$ and the capture by CoASH at $100\ s^{-1}$ (*22*). The presence and absence of CoASH has almost no effect on the first step. In the PheATE module, apoT vs holoT domain downstream has a ca. 2-fold effect on L-Phe-AMP formation rate.

For the aminoacyl-tRNA synthetases, e.g., Phe-tRNA synthetase (*23*, *24*), the L-Phe-AMP is captured not by a thiol nucleophile but by the 2′- or 3′-OH of the cognate tRNA. The aminoacyl-AMP formation rates are in the range of $20-60\ s^{-1}$, and the reverse hydrolysis rate constants vary from $15-200\ s^{-1}$, about 10-fold faster than these elementary steps in the GrsA module (*25*−*27*). The transfer rates of the aa-AMP to tRNA are typically slower than the first step, at $0.07-30\ s^{-1}$ (*21*, *25*, *26*), perhaps reflecting lower nucleophilicity of the oxygen vs sulfur atoms as attacking reagents. Also a slower second step may facilitate kinetic editing and fidelity checks in the aminoacyl-tRNA synthetase when a misacylated aa-AMP is formed (*27*). No evidence of proofreading has yet been seen in the NRPS adenylation-thiolation paired domains, not surprising given that there is relatively little consequence to incorrect amino acid incorporation into nonribosomal peptide antibiotics and siderophores (*11*, *15*).

The E domain at the C terminus of the A-T-E initiation module may exert a second gate keeper function after the A domain selection in gramicidin chain initiation. The antibiotic has a sequence D-Phe_1-L-Pro_2-L-Val_3-L-Orn_4-L-Leu_5, and the condensation domain in the ProCAT module, responsible for making the first peptide bond is strongly selective for D-Phe-S-Ppant-enzyme as the donor substrate (*8*, *28*, *29*). An inactive E domain, such as the H753A mutant (*8*), could not transfer D-Phe so chain growth is stalled. This would seem to put a premium on having the E domain function fast enough to not limit antibiotic chain growth. The rapid quench studies starting both from L-Phe as substrate and from D-Phe arrive at convergent values for the rate constants for interchange of L- and D-Phe-S-Ppant-enzyme of $1.8\ s^{-1}$ and $2.7\ s^{-1}$. The approach to equilibrium from both directions, L-Phe-S-Ppant-enzyme → D-Phe-S-Ppant-enzyme and D-Phe-S-Ppant-enzyme → L- Phe-S-Ppant-enzyme, gives the same numbers and the same 60/40 split of D-Phe-/L-Phe-S-Ppant-enzyme, suggesting that the bound Phe Cα-H configuration equilibrium and the E domain active site chiral microenvironment favors a slight accumulation of D-Phe over the 50/50 value. The ca. $2.5\ s^{-1}$ rate constant for flux of L-Phe-S-Ppant-enzyme → D-Phe-S-Ppant-enzyme is about 1500-fold faster than the observed peptide bond condensation rate for D-Phe-L-Pro-S-ProCAT module formation (*8*). Thus, the E domain is fast enough not to be a kinetically significant barrier in chain initiation/elongation and replenishes the D-Phe-S-T species that is drawn off for downstream transfer in a rapid preequilibrium. It will be of interest to determine if this is a general strategy in NRPS assembly lines with E domains embedded in elongation modules. The C domain downstream of such E domains should be D-specific for the donor peptidyl chain at the P1 position and the E domain should preequilibrate L-peptidyl- and D-peptidyl-S−T domain acyl enzyme forms.

ACKNOWLEDGMENT

We thank Dr. Petr Kuzmic, Dr. Perry Frey and Adrian D. Hegeman for helpful advice on the use of program DYNAFIT. Debbie A. Miller, Dr. Christopher Gary Marshall, Dr. Tom Keating, Dr. Huawei Chen, and Dr. Michael Thomas are gratefully acknowledged for a careful reading of the manuscript.

REFERENCES

1. Rapaport, E., Remy, P., Kleinkauf, H., Vater, J., and Zamecnik, P. C. (1987) *Proc. Natl. Acad. Sci. U.S.A. 84*, 7891−7895.
2. Lipmann, F. (1980) *Adv. Micro. Physiol. 21*, 227−266.
3. Kleinkauf, H., and Gevers, W. (1969) *Cold Spring Harbor Symp. Quant. Biol 34*, 805−813.
4. Kratzschmar, J., Krause, M., and Marahiel, M. A. (1989) *J. Bacteriol. 171*, 5422−5429.
5. Krause, M., and Marahiel, M. A. (1988) *J. Bacteriol. 170*, 4669−4674.
6. Stein, T., Kluge, B., Vater, J., Franke, P., Otto, A., and Wittmann-Liebold, B. (1995) *Biochemistry 34*, 4633−4642.
7. Stachelhaus, T., and Marahiel, M. A. (1995) *J. Biol. Chem. 270*, 6163−6169.
8. Stachelhaus, T., and Walsh, C. T. (2000) *Biochemistry 39*, 5775−5787.
9. Stein, T., Vater, J., Kruft, V., Otto, A., Wittmann-Liebold, B., Franke, P., Panico, M., McDowell, R., and Morris, H. R. (1996) *J. Biol. Chem. 271*, 15428−15435.
10. Conti, E., Stachelhaus, T., Marahiel, M. A., and Brick, P. (1997) *EMBO J. 16*, 4174−4183.
11. Stachelhaus, T., Mootz, H. D., and Marahiel, M. A. (1999) *Chem. Biol. 6*, 493−505.
12. Lambalot, R. H., Gehring, A. M., Flugel, R. S., Zuber, P., LaCelle, M., Marahiel, M. A., Reid, R., Khosla, C., and Walsh, C. T. (1996) *Chem. Biol. 3*, 923−936.
13. Quadri, L. E. N., Weinreb, P. H., Lei, M., Nakano, M. M., Zuber, P., and Walsh, C. T. (1998) *Biochemistry 37*, 1585−1595.
14. Schall, O. F., Suzuki, I., Murray, C. L., Gordon, J. I., and Gokel, G. W. (1998) *J. Org. Chem. 63*, 8661−8667.
15. Keating, T. A., Suo, Z., Ehmann, D. E., and Walsh, C. T. (2000) *Biochemistry 39*, 2297−2306.

16. Ehmann, D. E., Shaw-Reid, C. A., Losey, H. C., and Walsh, C. T. (2000) *Proc. Natl. Acad. Sci. U.S.A. 97*, 2509−2514.
17. Kuzmic, P. (1996) *Anal. Biochem. 237*, 260−273.
18. Linne, U., and Marahiel, M. A. (2000) *Biochemistry 39*, 10439−10447.
19. Cane, D. E., Walsh, C. T., and Khosla, C. (1998) *Science 282*, 63−68.
20. Chang, K. H., Xiang, H., and Dunaway-Mariano, D. (1997) *Biochemistry 36*, 15650−15659.
21. Fersht, A. (1999) *Structure and Mechanism in Protein Science*, W. H. Freeman and Co., New York.
22. Chang, K. H., and Dunaway-Mariano, D. (1996) *Biochemistry 35*, 13478−13484.
23. Sampson, J. R., Behlen, L. S., DiRenzo, A. B., and Uhlenbeck, O. C. (1992) *Biochemistry 31*, 4161−4167.
24. Reshetnikova, L., Moor, N., Lavrik, O., and Vassylyev, D. G. (1999) *J. Mol. Biol. 287*, 555−568.
25. Lin, S. X., Baltzinger, M., and Remy, P. (1984) *Biochemistry 23*, 4109−4116.
26. Pope, A. J., Lapointe, J., Mensah, L., Benson, N., Brown, M. J., and Moore, K. J. (1998) *J. Biol. Chem. 273*, 31680−31690.
27. Fersht, A. R., and Dingwall, C. (1979) *Biochemistry 18*, 1238−1245.
28. Ehmann, D. E., Trauger, J. W., Stachelhaus, T., and Walsh, C. T. (2000) *Chem. Biol. 7*, 765−772.
29. Belshaw, P. J., Walsh, C. T., and Stachelhaus, T. (1999) *Science 284*, 486-489.

BI015518+